



Measurements of Ultrafine Particles at Facades in Copenhagen

Description and comparison to Google Air View Data



Scientific Report

2023

Prepared by the Environmental Epidemiology Group

University of Copenhagen

Measurements of Ultrafine Particles at Facades in Copenhagen

Marie L. Bergmann

Zorana J. Andersen

Steffen Loft

Thomas Cole-Hunter

Youn-Hee Lim

Heresh Amini

Section of Environmental Health

Department of Public Health

University of Copenhagen

March 2023

Photo on title page: Branislav Nenin

Table of Contents

List of abbreviations	1
1. Introduction	2
2. Google Air View-based mixed model for UFP in Copenhagen	3
2.1 Methods	3
2.2 Results.....	4
3. Facade measurements of UFP in Copenhagen.....	6
3.1 Methods	6
3.2 Results.....	11
4. Comparison of UFP based on Google Air View and facade measurements	16
4.1 Methods	16
4.2 Results.....	17
5. Discussion	22
6. Conclusions	28
Acknowledgements	28
References	29

List of abbreviations

AMean-PNC Annual mean PNC at residential sites

CAV Copenhagen Air View Data

DiSCmini Handheld nanoparticle counter 'DiSCmini', manufactured by Testo

LUR Land-use regression

NO₂ Nitrogen dioxide

PM Particulate matter (particles)

PM_{2.5} Particulate matter of diameter <2.5 μm

PNC Particle number concentration

SD Standard deviation

SMPS Scanning Mobility Particle Sizer

UFP Ultrafine particles

WHO World Health Organization

1. Introduction

Ambient air pollution is a threat to human health worldwide, being responsible for more than six million premature deaths every year (1), and 4,200 premature deaths in Denmark (2). Health effects of air pollution include an increased risk of illness and death from ischemic heart disease, lung cancer, chronic obstructive pulmonary disease, lower-respiratory infections, stroke, type 2 diabetes, and adverse birth outcomes (3). Extensive research has been conducted especially on the health burden related to particulate matter of diameter $<2.5 \mu\text{m}$ ($\text{PM}_{2.5}$) (3,4), whereas increasing evidence today suggests that ultrafine particles (diameter $<0.1 \mu\text{m}$, UFP) may contribute significantly to this burden (5,6). Their increased toxicity is related to their large surface-area to mass ratio and their ability to carry relatively large quantities of potentially toxic compounds per unit volume (7). Moreover, UFPs' small size allows them to penetrate deep into the lungs and translocate into the bloodstream, reaching the body's different organs, and causing oxidative stress and inflammation, which are both associated with cardiovascular and respiratory diseases (8).

Unlike larger particles such as $\text{PM}_{2.5}$, UFP are not regulated or commonly monitored. They contribute little to particle mass concentration, the most widely used particle metric for particulate matter, and are thus not captured by routine monitoring. Instead, UFP are commonly measured as total particle number concentration (PNC) defined as the total number of particles per unit volume of air, which are dominated by particles in the ultrafine range (9). Within populated areas, sources of UFP are mainly of anthropogenic nature, related to the combustion of fossil- and biofuels as well as biomass, with road traffic being the most dominant source in urban areas, along with industrial sources, power plants, residential heating and biomass burning (9). Life spans of UFP in the air are shorter and exposure typically fluctuates more than for $\text{PM}_{2.5}$, with temporal variation and substantial differences between locations within the same city. Concentrations with the closest proximity to a source can be multiple times higher compared to those of urban background levels, but progressively revert to background levels in a short distance away from the source (10,11). In urban areas, mean background UFP concentrations of around $10,000 \text{ pt}/\text{cm}^3$ can be expected, while hourly mean concentrations can reach $20,000 \text{ pt}/\text{cm}^3$ (11).

Fine scale exposure data, ideally reflecting long-term mean concentrations at people's homes, is needed for epidemiological studies on the health effects of air pollution. Land-use regression (LUR)-modeling is a common method for exposure assessment of air pollutants, which has

recently increasingly be used for modelling UFP (12–20). Typically, LUR-models are developed based on a network of monitoring sites and a set of predictor variables from Geographic Information Systems (GIS) explaining variations in observed concentrations (21). A recent study by Kerckhoffs, Khan and colleagues (22) developed a mixed-effects model, called Copenhagen Air View Data (CAV), for street-level PNC in Copenhagen, using a combination of week-day and day-time repeated mobile monitoring by a Google Street View car from October 2018 to March 2020 in Copenhagen, and LUR-methods. This model adds a valuable additional contribution to existing knowledge on the spatial distribution of UFP in the Copenhagen area from monitoring and modelling (23,24). While its fine resolution and extensive mobile monitoring make the CAV-model attractive for possible utilization in epidemiological studies, if this model is to be used for residential exposure assessment, it is necessary first to evaluate its performance using residential measurements or comparison with other available model predictions. Previously, a national model developed for the Netherlands combining mobile monitoring with long-term regional background monitoring has shown good correlations with long-term external measurements (25). The CAV has previously been compared to UFP data from the Danish Air Quality Monitoring Program’s monitoring stations, as well as to address-level estimations of UFP from a Danish dispersion model (26). While emphasizing the limited comparability due to different methods, the CAV-model seems to overestimate concentrations at fixed-site monitoring stations, while no correlation was found between CAV and dispersion model estimations of UFP throughout the city.

In this report, to further our understanding of the CAV-model before possibly using it in epidemiological studies, we aimed to compare CAV-modelled concentrations of UFP to the UFP levels at the residences reflecting people’s exposure to UFPs at home, which we evaluated in a monitoring campaign at 37 residences in Copenhagen in two periods (warm and cold) during 2021-2022. In this report we first describe the CAV-model, our facade-level monitoring campaign, and UFPs concentrations from these two approaches.

Google Air View-based mixed model for UFP in Copenhagen

2.1 Methods

A detailed description of the monitoring and modelling processes behind the CAV-model can be found elsewhere (22,27). In short, monitoring was done by a Google Street View car, which was equipped with fast-response air quality monitoring instruments, and monitored PNC at 1-second intervals on every street in Copenhagen, Frederiksberg and Tårnby municipalities from

October 15, 2018, to March 15, 2020. The number of drive days per street segment ranged from 1 to 126, with a mean of 7 drive days per street segment. Monitoring was done between 08:00 and 22:00 h on weekdays, with most measurements between 10:00 and 16:00 h. PNC monitoring was done using a water-based CPC (EPC 3783, TSI) with a lower detection limit at 7 nm. First, a LUR-model was developed with an R^2 of 0.36. LUR-model predictors were several indicators of traffic intensity, area of airports in a 5,000-m buffer, area of ports in a 1,000-m buffer, area of industry in a 5,000-m buffer, and area of water in a 1,000-m buffer (22,27). The predictors of the LUR-model were then used as fixed effects in a mixed-effects model with random intercepts for all individual street segments (N=30,312). The data is available at <https://insights.sustainability.google/labs/airquality>.

2.2 Results

Figure 1 shows CAV-model predictions of PNC for all streets in Copenhagen, Frederiksberg and Tårnby municipalities. Predicted concentrations have a large range of 3,340 to 65,600 pt/cm^3 . Elevated concentrations are observed in the eastern part of Amager in the area around the airport, as well as on major roads, such as the E20 highway crossing Amager. Lowest concentrations are observed in residential areas away from major roads or the airport.

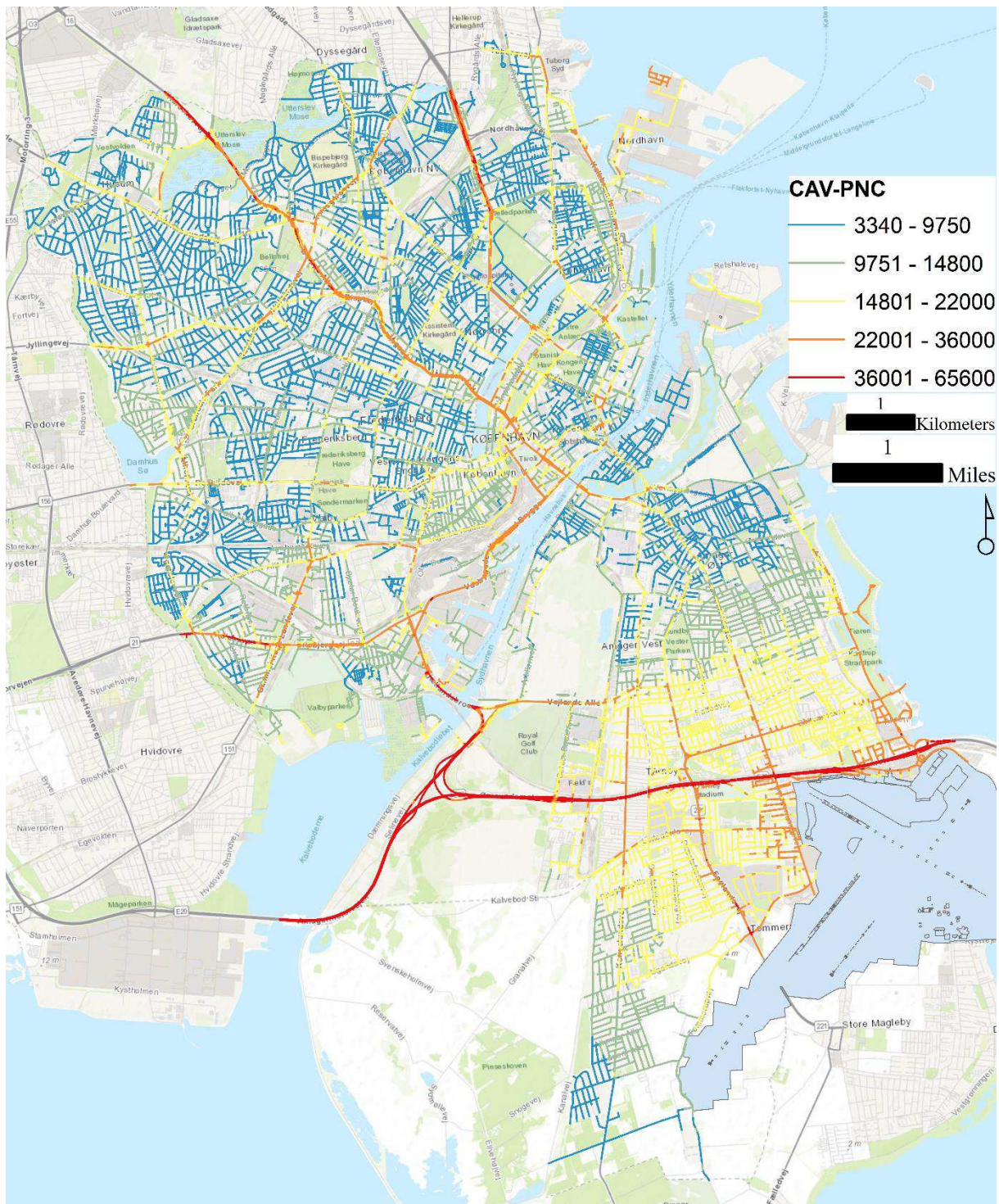


Figure 1. Spatial distribution of PNC on streets in Copenhagen, Frederiksberg and Tårnby municipalities based on CAV.

2. Facade measurements of UFP in Copenhagen

3.1 Methods

Measurement campaign

We conducted a measurement campaign of 37 residences in Copenhagen, Frederiksberg and Tårnby municipalities with an area of ca. 255 km² (Figure 2), and a reference site in central Copenhagen, from May 29, 2021, to May 29, 2022. Volunteers were recruited opportunistically, with a focus on a spatially representative distribution of locations across the study area. Measurements were done continuously at the reference site for about one year, and additionally across the 37 city-wide distributed residences either Monday-Thursday or Thursday-Monday (~72 hours), twice at each location in two campaigns. Campaign 1 was from July 08 to November 08, 2021, and Campaign 2 was from February 10 to May 29, 2022. The objective of having a reference site and two campaigns was to use the reference site for temporal adjustment of city-wide measurements to approximate the annual mean at each site, similar to other studies (28,29). The monitoring period was not significantly impacted by societal closures in response to the Covid-19-pandemic (30).

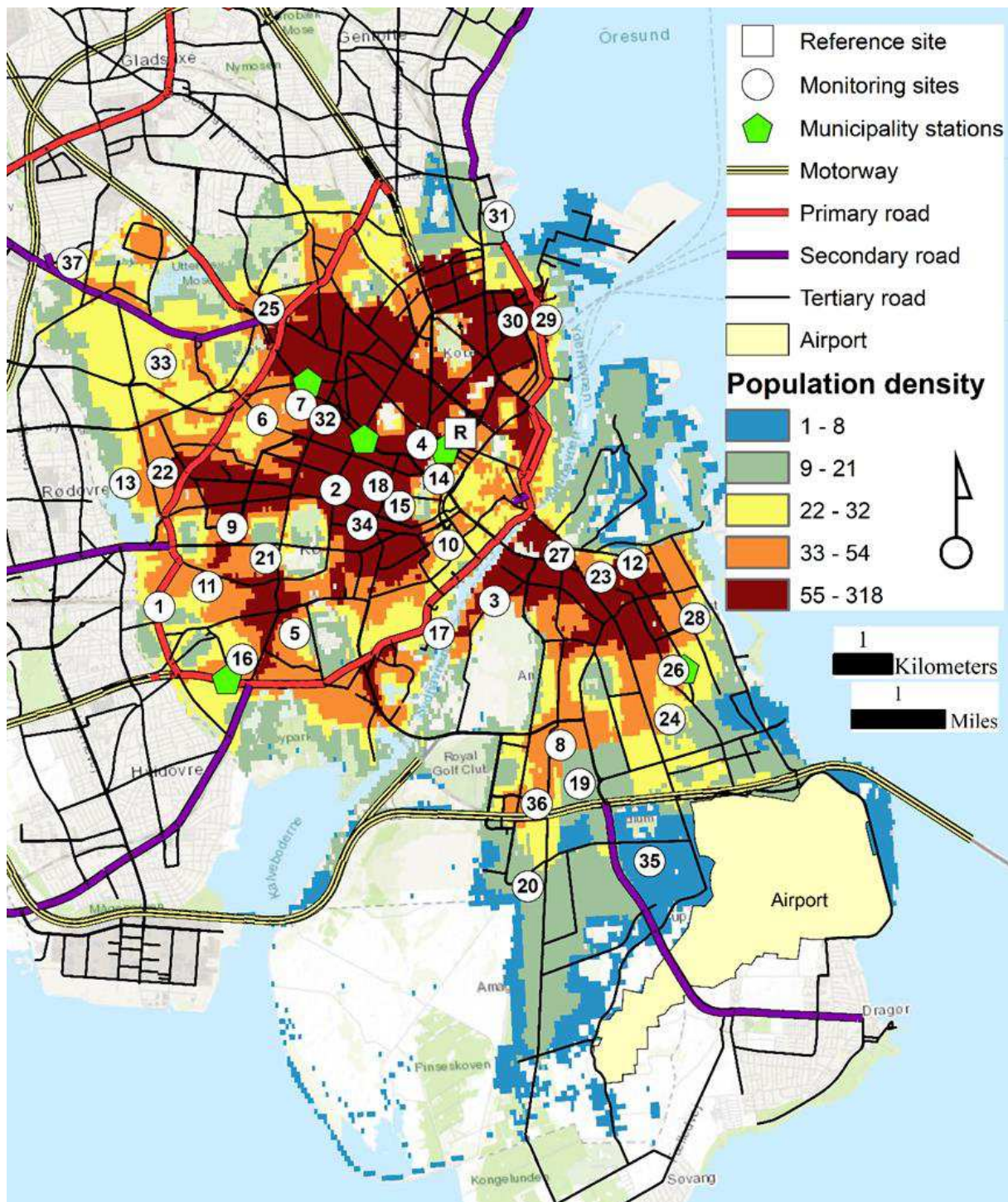


Figure 2. Location of 37 residential monitoring sites, reference site (“R”), and five municipality monitoring stations, with underlying colors indicating population density in the study area.

We used miniature diffusion size classifiers (‘DiSCmini’ [DM]; Testo SE & Co. KGaA, Germany) to measure PNC, as well as particle diameter in nanometers (nm), at 1-s intervals. The DM measures particles within a diameter range of 10–300 nm (modal diameter) with an impactor for particle size cut-off at 700 nm, and PNC range of 1,000 to 1,000,000 particles per cubic centimeter of air (pt/cm³). We additionally used a flexible, manufacturer-provided

polymer sampling tube as an extension between the instrument and impactor. The instruments were set up in weather-proof plastic boxes on windowsills or balconies, on ground or first floor level, or in house entrances, facing the street wherever possible, such as to represent concentrations immediately close to the residences (see Figure 3 for example setup). At the reference site, a DM monitored PNC and particle diameter continuously for one year (May 29, 2021, to May 29, 2022), located in a courtyard at a University of Copenhagen campus, mostly free from traffic contributions. The instrument was placed in a box attached to a building facade at about four meters height. Data of each measurement was stored as text files on SD cards and processed in manufacturer-provided computer software, where it was averaged to minute-intervals prior to further data cleaning.



Figure 3. Exemplary measurement setup at a volunteer's residence.

Meteorological information, as hourly means of temperature and relative humidity, was obtained from a monitoring site located in central Copenhagen. Monitoring of meteorological data at this site was discontinued after March 2022, thus meteorological data for the last two

months of our monitoring campaign (April and May) was obtained from the Danish Meteorological Institute.

Quality Assurance and Quality Control (QAQC)

A total of four DM instruments were used for this study, which were either newly purchased or recently calibrated. The manufacturer recommends annual calibration for DMs. However, since we operated them intensively, we sent them to Testo for re-calibration after Campaign 1, before using them again in Campaign 2.

According to manufacturer recommendation, ‘zero checks’ were performed immediately before and after DM measurements using a HEPA filter. Zero checks at the reference site were done weekly, including cleaning of the impactor, following the instrument manual. Protocols were in place in order to assure consistent instrument setup and operation.

To evaluate the accuracy of DM instruments, we co-located our instruments at a regulatory air quality monitoring station in central Copenhagen (H.C. Andersens Boulevard) on three occasions: one week directly after each of the two monitoring campaigns (“Co-location 1”: November 09-17, 2021, and “Co-location 2”: May 31-June 07, 2022), as well as an additional period of two weeks (“Co-location 3”: August 23-September 06, 2022). The regulatory monitoring station is equipped with a Scanning Mobility Particle Sizer (SMPS), which counts particles with mobility diameters between 11 and 478 nm. The hourly mean PNC by DMs and SMPS were compared to examine the accuracy of DM measurements.

Furthermore, to evaluate the accuracy of our measurements at the reference site, we obtained publicly available data for the same year as our monitoring campaign (May 29, 2021-May 29, 2022) from five street-level monitoring stations by the municipality of Copenhagen (available at <https://erluftensund.kk.dk/maaling-og-maalestationer>), and compared our daily mean values with those from each of these five sites. The sites are located immediately next to streets (sidewalks) across the city (Figure 2), with low to high traffic intensity, ranging from 3,276 to 52,650 daily traffic counts. They report hourly PNC, using a GRIMM 5421 condensation particle counter (CPC) with a lower detection limit at 7 nm.

To evaluate the precision of DM instruments, we co-located the DMs and compared absolute levels of hourly mean PNC with each other at the regulatory monitoring station on the same

occasions as described above. We also assessed correlation of hourly means between DM instruments.

Lastly, we developed the following algorithm for data cleaning of minute-averaged data, inspired by previous studies (28), as well as recommendations for instrument operation by the DM manufacturer.

1. Remove data points if the particle diameter was outside manufacturer-given range of 10-300 nm.
2. Remove data points if the 1-minute average of PNC was outside manufacturer-given detection range of 1,000-1,000,000 pt/cm³.
3. Truncate the 1-minute averages of PNC to the 99th percentile of all data points (i.e., replace the values above 99th percentile by the 99th percentile value).
4. Remove data points if the instrument's flow was below 0.9.
5. Remove data points if values in the diffusion or filter stage were negative.
6. Remove data points if ambient hourly mean ambient air temperature exceeded 30°C or relative humidity exceeded 90%, which are outside of the manufacturer-given recommendations for optimal DM operation.

Statistical analysis

All analyses were done in R statistical software (v 4.1.1; R Core Team, Vienna, Austria) and ArcGIS (v 10.8.1; ESRI, Redlands, CA).

To approximate the annual mean of PNC (AMean-PNC) at each of the 37 sites using two short-term measurement campaigns, temporal adjustment was done using data of the reference site, according to commonly used ratio and difference methods (31,32). These methods are based on the assumption that the difference of annual means between two locations (i and j as examples) within a city typically remains similar throughout the year. If the annual mean is available at location i , and short-term samples are done in location j , the difference between the simultaneous measurements in these two locations should also remain similar. However, meteorology and other factors may affect this difference (or ratio), thus repeated samples in colder and warmer seasons (or across four seasons) are suggested.

We implemented a simulation with one-year data from five municipality monitoring stations to find the best temporal adjustment method. Equations 1 to 3 present formulas for a difference-, ratio-, and combined method for temporal adjustment. In equation 1 and 2, each site measurement from either campaign provided an estimate for annual mean PNC. As we had two

measurements at most sites, the two annual estimations provided by each temporal adjustment method were then averaged to provide a better estimation of the site's annual mean. Based on our simulation, the combined method (Equation 3) performed best and was therefore used for temporal adjustment of our measurements. The main analyses were made only with the sites that had two valid measurements (in Campaign 1 and 2) and corresponding reference site values because our simulation showed that annual mean calculation based on one measurement can result in considerable error.

$$\text{Site (annual)}_{diff} = \text{Site (~72hours)} + \{\text{Reference (annual)} - \text{Reference (~72hours)}\} \quad (1)$$

$$\text{Site (annual)}_{ratio} = \text{Site (~72hours)} \times \{\text{Reference (annual)} \div \text{Reference (~72hours)}\} \quad (2)$$

$$\text{Site (annual)}_{comb} = 0.5 \times \{\text{Site (annual)}_{diff} + \text{Site (annual)}_{ratio}\} \quad (3)$$

Data from the three co-locations of DMs at a regulatory monitoring station was analyzed by applying the same data cleaning steps for DMs as described above and subsequently merging hourly means of DM and SMPS. We then applied Spearman's correlation between DMs, as well as between DMs and SMPS. For comparison with our reference site, daily mean PNC from the five municipality monitoring stations was merged with daily means at the reference site, and Spearman's correlation was assessed.

3.2 Results

Description of measurement campaign

During one year (May 29, 2021 to May 29, 2022), 7,567 hours of data were collected at the reference site, of which ~30% were subsequently removed during the data cleaning process. This was mostly related to instrument pump malfunctions for several weeks during summer (June and July) and a period of two weeks in December-January, where a software error made output files unreadable. While we started with 37 volunteer residences, we were only able to conduct two valid measurements at 27 sites (Table 1), with nine remaining sites having only one valid measurement.

Table 1. Description of 37 residential measurement sites.

Site ID	N of valid measurements *	Traffic counts on nearest street**	Distance to major road (m)	Distance to Google road (m)	Within airport vicinity (<5 km)	Floor number (0=ground floor)	Monitor facing street
Reference	N/A	23,868 (4)	85	83	No	1	No
1	2	16,146 (4)	91	22	No	0	Yes
2	2	17,250 (4)	17	20	No	1	Yes
3	1 (W)	12,051 (4)	19	16	Yes	0	Yes
4	0	199 (1)	230	104	No	1	Yes
5	2	2,574 (3)	302	10	No	1	Yes
6	2	12,519 (4)	16	14	No	1	Yes
7	2	2,054 (2)	260	7	No	0	No
8	2	10,296 (4)	187	15	Yes	0	Yes
9	2	8,835 (3)	108	10	No	1	Yes
10	2	1,088 (1)	75	14	No	1	Yes
11	1 (W)	11,466 (4)	231	16	No	0	No
12	1 (S)	3,978 (3)	41	14	Yes	1	Yes
13	2	1,170 (2)	452	15	No	0	Yes
14	1 (S)	2,176 (2)	37	18	No	1	Yes
15	2	1,440 (2)	265	15	No	0	Yes
16	1 (S)	1,088 (1)	279	51	No	1	Yes
17	1 (W)	1,100 (1)	72	76	No	0	Yes
18	2	5,805 (3)	165	7	No	0	Yes
19	2	1,155 (2)	317	15	Yes	0	Yes
20	2	2,340 (2)	162	30	Yes	0	Yes
21	1 (W)	9,297 (3)	203	25	No	0	Yes
22	2	1,170 (2)	152	18	No	1	Yes
23	1 (W)	3,510 (3)	49	29	Yes	1	Yes
24	2	1,088 (1)	334	5	Yes	0	Yes
25	2	1,100 (1)	190	30	No	1	Yes
26	2	8,775 (3)	152	11	Yes	0	Yes
27	2	17,550 (4)	14	5	Yes	0	Yes
28	2	117 (1)	89	5	Yes	0	Yes
29	2	1,100 (1)	108	129	No	1	Yes
30	2	491 (1)	137	15	No	1	Yes
31	2	15,561 (4)	81	15	No	0	Yes
32	1 (S)	1,149 (2)	97	5	No	0	Yes
33	2	11,232 (4)	430	39	No	0	Yes
34	2	8,097 (3)	45	11	No	1	Yes
35	2	1,176 (2)	331	45	Yes	0	No
36	2	1,088 (1)	178	40	Yes	0	No
37	2	19,071 (4)	126	15	No	0	Yes
Summary	'0': 1 (3%) '1': 9 (24%) '2': 27 (73%)	Mean: 6,320 '1': 10 (27%) '2': 9 (24%) '3': 8 (22%) '4': 11 (30%)	Mean: 161	Mean: 27	'Yes': 11 (30%) 'No': 26 (70%)	'0': 21 (57%) '1': 16 (43%)	'Yes': 32 (86%) 'No': 5 (14%)
<p>*If only one measurement was done, (S) or (W) indicates, whether this was done in Campaign 1 (summer) or Campaign 2 (winter), respectively.</p> <p>**Traffic counts are based on the annual average of daily number of vehicles on the nearest street in 2017. Categories are based on quartiles: 1=0-1112; 2=1113-2340; 3=2341-9547; 4=9548+ daily traffic counts.</p>							

For five sites in Campaign 1, corresponding reference data was not available for monitoring dates, due to problems with the instrument's pump during some summer weeks. Additionally, five sites (one of them overlapping with the previously mentioned five sites) were not included in Campaign 2 due to different reasons, including construction of building facades or moving of the participants, leading to a final number of 36 sites, which had at least one valid measurement and corresponding ratio/difference to the reference site. Monitoring sites were located, on average, within 27 m from the nearest road with Google Street View measurements, within 161 m from major roads, and with daily traffic counts between 117 and 19,071. Eleven sites were located within a 5 km radius from the airport. Site measurements were mostly done facing the street (86% of sites) and on the ground floor (57%). The proportion of sites monitored either Monday-Thursday or Thursday-Monday was about equal in both campaigns. For more than half of the sites (60%), both measurements were done on the same combination of days of the week, while 40% of sites had one of each combination. The mean temperature in Campaign 1 (July-November) was 14°C, and 8°C in Campaign 2 (February-May). We collected 3,019 hours of data at residential monitoring sites in Campaign 1, and 2,719 hours in Campaign 2, of which 11% and 13% were subsequently removed during data cleaning, respectively. For each monitoring site, the final dataset included 72 hours of data, on average, in Campaign 1, and 76 hours in Campaign 2, ranging between 31-103 and 47-98 hours of monitoring at individual sites per campaign, respectively. Hourly mean PNC at monitoring sites and reference site were well correlated, with Spearman's correlation coefficients of 0.74 (25th-75th percentile: 0.62-0.85) and 0.73 (0.65-0.81) in Campaign 1 and 2, respectively.

QAQC results

Three co-locations at a regulatory air quality monitoring station showed acceptable repeatability of DM measurements. However, only two out of three DMs' data could be used during each of the co-locations, due to malfunctions of instruments beginning either during or immediately before the co-locations. Hourly mean PNC of two DMs was compared with each other for 132, 122 and 71 hours (after data cleaning) in Co-location 1, 2, and 3, respectively, where Spearman's correlation coefficients ranged between 0.96 and 0.99. Absolute levels of PNC were in good to moderate agreement, with differences of 6%, 7% and 22% in respective co-locations (Table 2).

Table 2. Particle number concentration and diameter of three DMs and SMPS during three co-locations at a regulatory monitoring station (09-17 Nov 2021, 31 May-07 June 2022, and 23 August-06 September 2022).

	Instrument	Mean	SD	Min-Max	Percentiles			
					25 th	50 th	75 th	95 th
Co-location 1^a								
PNC (pt/cm ³)	DM 1	15,496	10,333	1,668-56,670	9,602	13,713	19,215	37,895
	DM 4	14,632	9,948	1,635-55,471	8,833	12,835	17,417	35,869
	SMPS	8,826	5,322	889-29,333	5,414	8,052	11,368	19,213
Diameter (nm)	DM 1	42	11	26-76	33	39	48	65
	DM 4	41	11	20-72	32	38	46	62
Co-location 2^b								
PNC (pt/cm ³)	DM 3	13,084	8,957	1,853-51,710	7,579	9,868	15,801	33,351
	DM 4	14,131	9,586	1,845-49,983	7,840	10,992	17,519	35,719
Diameter (nm)	DM 3	40	9	13-65	34	40	45	54
	DM 4	38	7	24-61	34	39	42	50
Co-location 3								
PNC (pt/cm ³)	DM 3	11,229	4,453	2,143-24,689	8,789	10,575	13,497	19,167
	DM 4	14,340	12,580	2,890-111,548	9,802	12,597	15,759	23,504
	SMPS	11,272	4,792	1,908-28,638	8,363	10,772	13,083	19,529
Diameter (nm)	DM 3	36	5	23-47	34	36	40	44
	DM 4	40	8	17-63	35	40	44	55
^a Co-location 1: DM 3 malfunction during entire co-location. ^b Co-location 2: DM 1 pump malfunction after 19 hours, so summary statistics are not comparable. SMPS data not available due to instrument malfunction. Note: SMPS data for 2022 (Co-location 3) is preliminary data before final quality control. Abbreviations: SD, standard deviation; Min, minimum; Max, maximum; PNC, particle number concentration; DM 1-4, DiSCmini instrument number 1-4.								

For the evaluation of accuracy, corresponding SMPS data was available for Co-location 1 and 3, but was, at the time of analysis, only preliminarily quality controlled for Co-location 3 dates. The two DMs were correlated with the SMPS at hourly averages with 0.92-0.93 in Co-location 1 and 0.77-0.82 in Co-location 3. Moreover, we found that DMs measured considerably higher PNC than the SMPS in Co-location 1, with about 66-76% higher hourly mean PNC by DMs compared to SMPS, while there was better agreement (1-27% higher) in hourly PNC between the instruments in Co-location 3 (Table 2).

Daily mean PNC at the reference site was highly correlated with that of five municipality street-level monitoring stations throughout the city. Spearman's correlation coefficients ranged between 0.83 and 0.84, with only one station correlated less well at 0.64. Annual means for May 2021 to May 2022 at the monitoring stations ranged from 5,590 to 7,600 pt/cm³, which is

considerably higher than 4,715 pt/cm³ at our reference site, but consistent with their traffic-oriented locations.

Description of facade-level annual mean PNC

Annual mean (SD of hourly averages) PNC at the reference site was 4,715 (3,001) pt/cm³ (Table 3), while annual means at the residential monitoring sites were slightly higher with a mean of 5,201 pt/cm³, ranging between 3,735 and 6,588 pt/cm³ at individual sites (Table 4). Campaign-specific mean PNC at residential sites was 4,860 (range: 2,110-7,711) in Campaign 1 and 6,843 (3,430-11,450) pt/cm³ in Campaign 2. These two values across 27 sites were correlated with 0.31 (Spearman’s correlation) and had an intra-class correlation coefficient of 0.10 (95%-confidence interval: -0.10, 0.34). Furthermore, they were correlated with the estimated annual mean at sites with 0.19 and 0.55 for Campaign 1 and Campaign 2, respectively.

Table 3. Summary statistics of hourly mean particle number concentrations monitored at the reference site.

	N (hours)	Mean	SD	Min-Max	Percentiles			
					25 th	50 th	75 th	90 th
Hourly PNC (pt/cm³)	5,375	4,715	3,001	1,005-17,821	2,558	4,096	5,996	8,487
Abbreviations: N, number of observations; SD, standard deviation; Min, minimum; Max, maximum; PNC, particle number concentration.								

Table 4. Summary statistics of measured facade-level particle number concentrations at residential monitoring sites.

	N (sites)	Mean	SD	Min-Max	Percentiles			
					25 th	50 th	75 th	90 th
Campaign-1-PNC (unadjusted, pt/cm³)	37	4,860	1,284	2,110-7,711	3,920	4,890	5,809	6,111
Campaign-2-PNC (unadjusted, pt/cm³)	32	6,843	1,788	3,430-11,450	5,646	6,483	7,692	7,044
AMean-PNC (pt/cm³)	27	5,206	807	3,735-6,588	4,703	5,114	5,737	6,362
Abbreviations: N, number of observations; SD, standard deviation; Min, minimum; Max, maximum; PNC, particle number concentration; AMean-PNC, estimated temporally adjusted annual mean.								

Highest concentrations at the reference site were seen in March-May, and lowest in November-January (Figure 4). At monitoring sites, PNC was generally higher in Campaign 2 than in Campaign 1, indicating a similar seasonal trend.

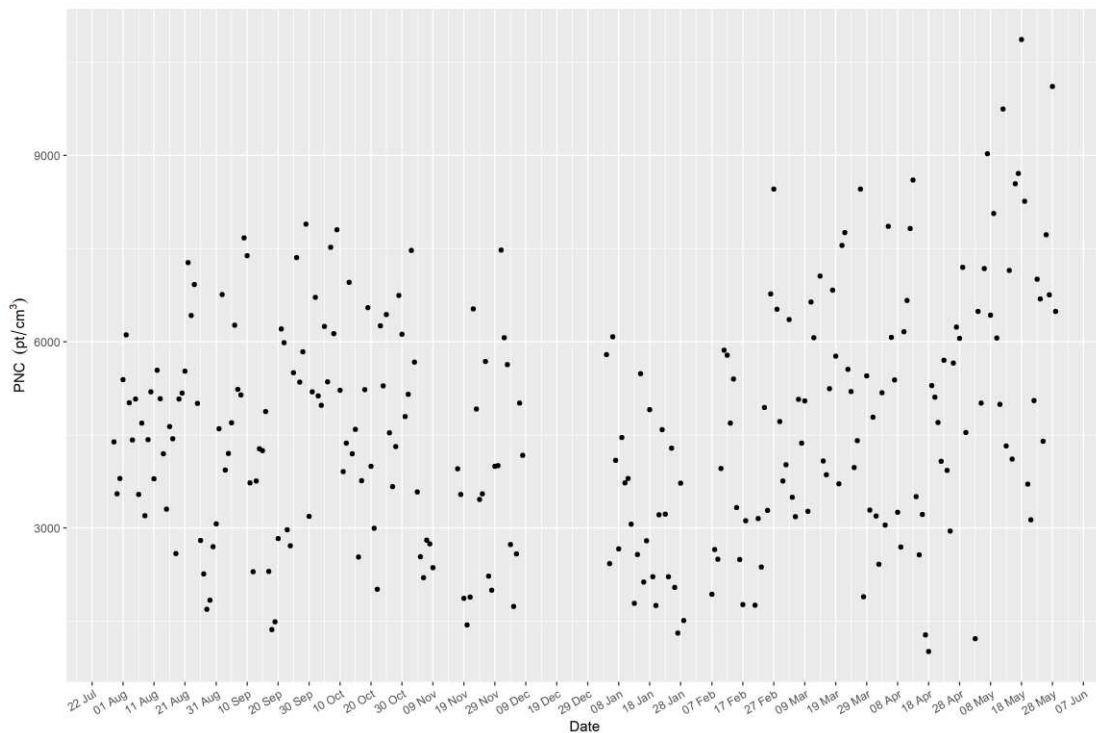


Figure 4. Daily averages of PNC at the reference site during one year (May 29, 2021-May 29, 2022).

3. Comparison of UFP based on Google Air View and facade measurements

4.1 Methods

As the CAV-model reports PNC values for each road segment in a polyline format, we first rasterized the predictions using the natural neighbor method with a 15 m cell size (33). This was preferred to linking the data from the nearest street, as residences are often surrounded by multiple streets, and the accurate exposure could be a composite value based on the data of nearby streets. Next, the PNC values were extracted for each of the 37 residences. In sensitivity analyses, we additionally extracted the nearest road segment’s prediction for each of the 37 residences without interpolation.

The main comparisons between measurements and model were made only with the 27 sites that had two valid measurements (in Campaign 1 and 2) and corresponding reference site values.

Differences between campaign-specific (Campaign-1-PNC and Campaign-2-PNC) and temporally adjusted AMean-PNC values at residential sites based on measurements and CAV-

model PNC predictions (CAV-PNC) were investigated by (1) Spearman's correlation, (2) coefficient of variation, (3) Bland-Altman plots between the above mentioned measures showing the differences of pairs versus their average values. The ideal Bland-Altman plot is where the points are symmetrically distributed around the zero-difference line, the cloud of the points has a zero slope, and the points have slight vertical variability within the limits of agreement (mean difference $\pm 2 \times \text{SD}$)).

We conducted several sensitivity analyses in the following steps: (1) include all sites regardless of the number of valid measurements, (2) restricting monitored data to week-days (Monday-Friday) and day-time hours (08-22 h), in accordance with Google Street View monitoring, (3) sites where CAV-PNC was based on at least five drive days of the Google Street View car (i.e., the mean of drive days at 37 monitoring sites), (4) log-transformed annual mean data, (5) based on distance to major roads for monitoring sites (i.e., motorways, important/primary/secondary/tertiary roads), (6) based on the level of PNC at sites, (7) based on measured mean particle size at the site, indicating different sources of particles.

4.2 Results

Mean (SD) CAV-PNC at 27 residential sites was 11,804 (5,423) pt/cm^3 , ranging from 4,422 to 30,956 pt/cm^3 . The coefficient of variation was 46 for CAV-PNC, while for AMean-PNC it was 16. Campaign-1-PNC at 37 sites, before temporal adjustment, was positively correlated with CAV-PNC (0.28) at corresponding addresses, while Campaign-2-PNC at 32 sites and CAV-PNC were correlated with 0.30 (Table 5 and Figure 5). A comparison of temporally adjusted AMean-PNC with CAV-PNC showed no agreement between the two values. Spearman's correlation between AMean-PNC (at 27 sites with two valid measurements and corresponding reference site data) and CAV-PNC was -0.01. Restricting monitored data to week-days and day-time increased correlation to a negative value of -0.14. In addition, we found that CAV-PNC was 2.5 times higher than AMean-PNC on average, ranging from 1.1 to 6.4 at individual sites. The results were similar, when CAV-PNC was assigned to addresses using the nearest road segment's value instead of natural neighbor interpolation (results not presented).

Table 5. Spearman's correlation matrix of campaign-specific PNC, annual mean PNC and CAV-PNC predictions at 27 residential monitoring sites.

	Campaign-1-PNC	Campaign-2-PNC	AMean-PNC	CAV-PNC
Campaign-1-PNC	1	0.31	0.19	0.28 ^a
Campaign-2-PNC	0.31	1	0.54	0.30 ^b
AMean-PNC	0.19	0.55	1	-0.01
CAV-PNC	0.28 ^a	0.30 ^b	-0.01	1

^a Based on unadjusted Campaign-1-PNC at 37 sites.

^b Based on unadjusted Campaign-2-PNC at 32 sites.

Abbreviations: AMean-PNC, estimated temporally adjusted annual mean; CAV-PNC, Google Air View-Mixed model PNC.

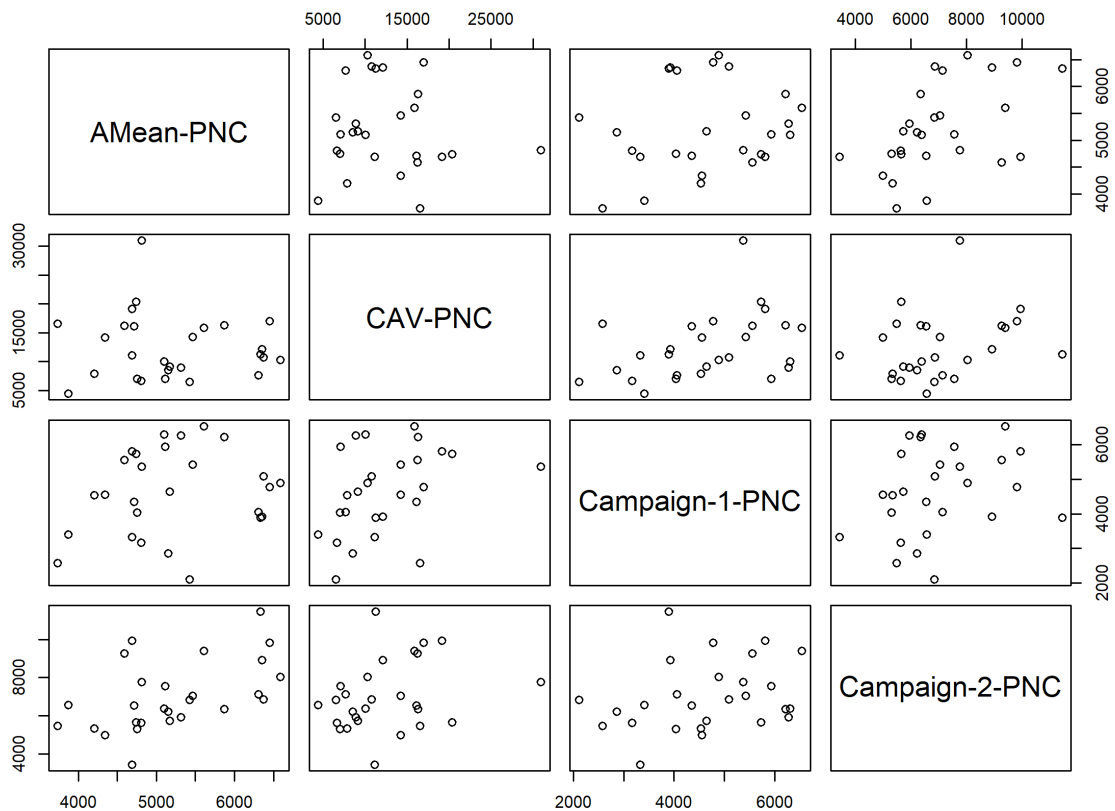


Figure 5. Scatterplot matrix of AMean-PNC, CAV-PNC, Campaign-1-PNC and Campaign-2-PNC at 27 sites.

A Bland-Altman plot (Figure 6) showed increasing differences between AMean-PNC and CAV-PNC with increasing PNC levels.

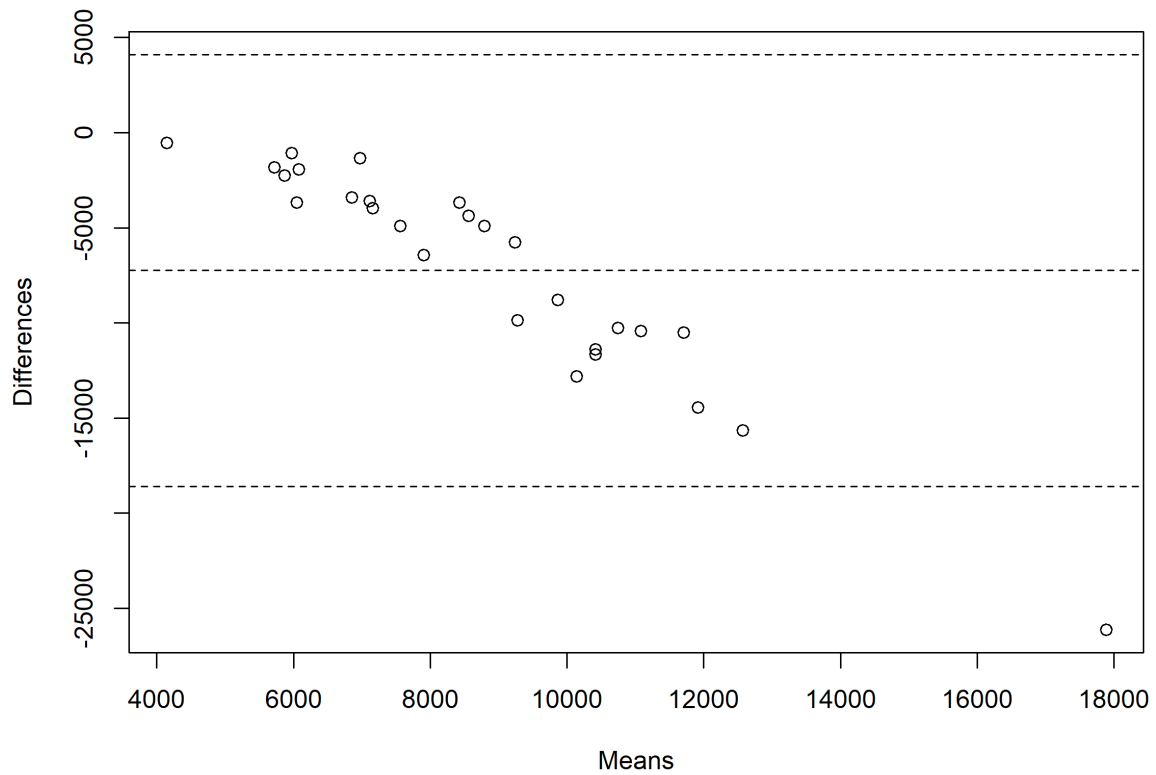


Figure 6. Bland-Altman plot of agreement between AMean-PNC and CAV-PNC at 27 monitoring sites with two complete observations, showing the differences of pairs versus their average values. The ideal plot is where the points are symmetrically distributed around the zero difference line, the cloud of the points has a zero slope, and the points have slight vertical variability within limits of agreement (Mean difference $\pm 2 \times$ SD).

There was no apparent spatial pattern for agreement between AMean-PNC and CAV-PNC (Figure 7). Higher AMean-PNC was seen closer to the center of Copenhagen, but also in some south-western and southern suburbs.

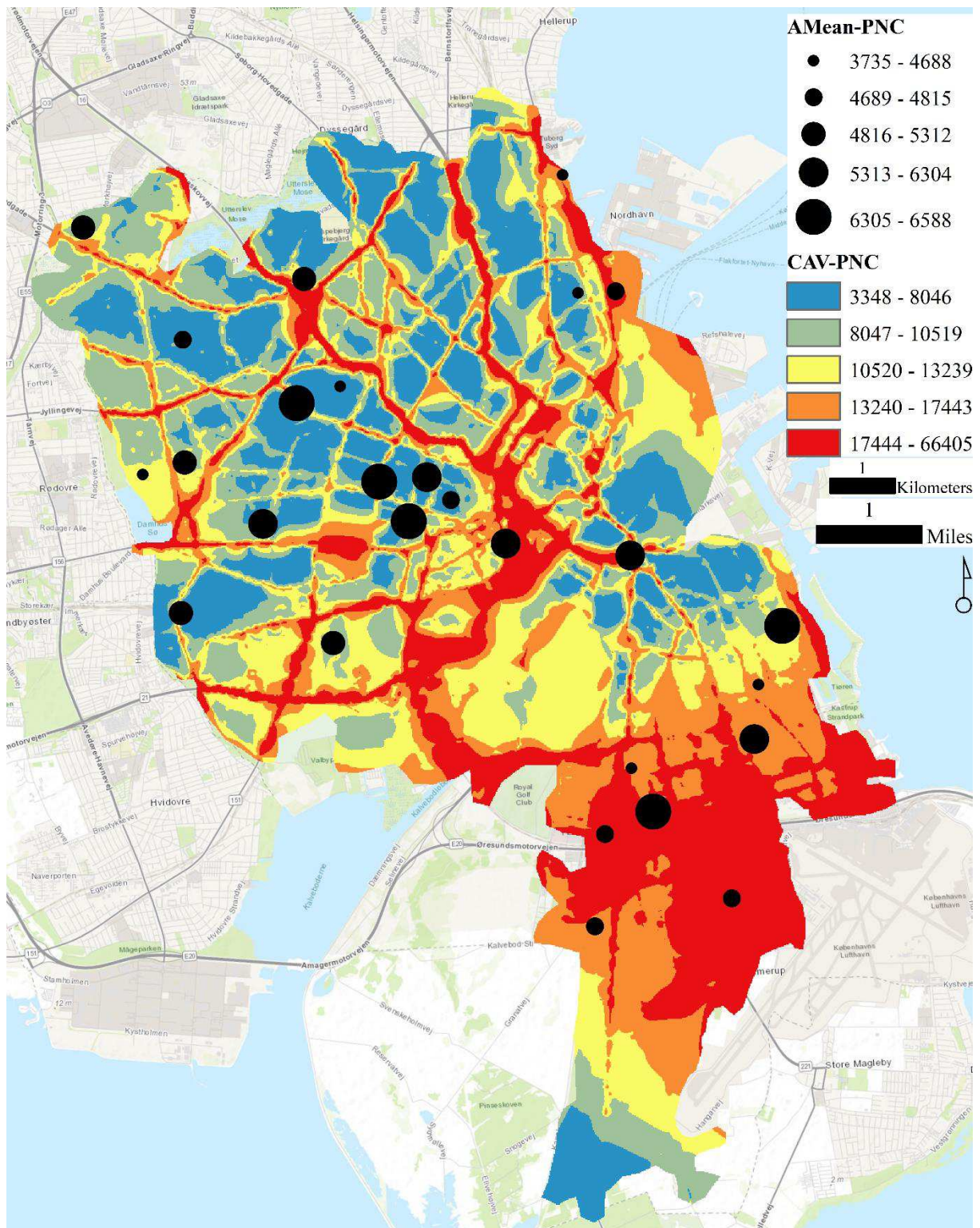


Figure 7. Interpolated CAV-PNC and measured AMean-PNC at 27 residential monitoring sites. Interpolated PNC was derived from CAV-model mid-road estimates across 30,312 streets using natural neighbor method with a cell size of 15 m.

In additional analyses, log-transformation of monitoring data was done to account for skewed data, but this did not change results significantly (Table 1). Several further analyses showed

that correlation between AMean-PNC and CAV-PNC was stronger and negative for street segments in mobile monitoring with more than five drive days (-0.43), and not substantially different for all 37 sites (additionally including those with only one out of two measurements), by distance to a major road, or for log-transformed data. Correlation was higher at sites with AMean-PNC above 5,000 pt/cm³ (0.54), and moderate with CAV-PNC below 10,000 pt/cm³ (0.36) or with mean particle diameter measured at the site below 45 nm (0.26). Those sites outside a 5 km radius from the airport had better correlation with CAV (0.17) compared to those close to the airport (-0.03).

Table 6. Spearman’s correlation of AMean-PNC with CAV-PNC at residential measurement sites: main analysis and sensitivity analyses.

	N (Sites)	Spearman’s rho (p-value)	Ratio of AMean- to CAV-PNC
Main analysis*	27	-0.01 (0.95)	0.50
All sites	36	-0.14 (0.42)	0.54
Sites with >5 drive days*	7	-0.43 (0.35)	0.50
Distance to major road*			
≤150 m	12	-0.06 (0.87)	0.52
>150 m	15	-0.01 (0.96)	0.48
Log-transformed data*	27	0.00 (0.97)	0.46
AMean-PNC at site*			
<5000 pt/cm ³	12	0.22 (0.50)	0.41
>5000 pt/cm ³	15	0.54 (0.04)	0.56
CAV-PNC at site*			
<10000 pt/cm ³	12	0.36 (0.31)	0.70
>10000 pt/cm ³	15	-0.33 (0.20)	0.38
Distance to airport*			
<5 km	9	-0.03 (0.95)	0.32
>5 km	18	0.17 (0.51)	0.59
Annual mean particle diameter at site *			
<45 nm	9	0.26 (0.47)	0.57
>45 nm	18	-0.07 (0.78)	0.46
Daytime (8-22 h), weekdays (Mon-Fri) means*	27	-0.14 (0.48)	0.53
All sites	36	-0.23 (0.18)	0.57
Sites with >5 drive days*	7	0.11 (0.84)	0.54
Distance to major road*			
≤150 m	12	0.06 (0.87)	0.56
>150 m	15	-0.31 (0.26)	0.50
Log-transformed data*	27	-0.11 (0.60)	0.49
AMean-PNC at site*			
<5000 pt/cm ³	12	-0.01 (0.97)	0.44
>5000 pt/cm ³	15	0.19 (0.51)	0.60
CAV-PNC at site*			
<10000 pt/cm ³	12	0.19 (0.61)	0.75
>10000 pt/cm ³	15	-0.38 (0.13)	0.40
Distance to airport*			
<5 km	9	-0.33 (0.39)	0.33
>5 km	18	0.17 (0.50)	0.63
Annual mean particle diameter at site*			
<45 nm	9	0.02 (0.97)	0.60
>45 nm	18	-0.12 (0.65)	0.48

* With two complete, valid measurements and corresponding ratios/difference with reference site.
Abbreviations: AMean-PNC, estimated temporally adjusted annual mean; CAV-PNC, Google Air View-Mixed model PNC.

4. Discussion

We conducted a monitoring campaign of facade-level PNC at 37 residential sites in the Copenhagen area and determined temporally adjusted annual mean PNC based on two valid measurements at 27 sites. Assessments of the reliability of our measurements with DMs showed that instruments had good precision, when co-located. Moreover, accuracy in terms of agreement with a SMPS at a regulatory air quality monitoring station showed mixed results, with high correlation, but disagreement of absolute PNC levels during one co-location. Our long-term measurements at a reference site were found to be in good agreement with five municipality monitoring stations of PNC at different locations throughout the city. Finally, estimated annual mean PNC based on our facade-level measurements at 27 residential sites was not correlated with PNC from CAV on the streets surrounding them (-0.01). Moreover, the CAV-model predicted 2.5 times higher PNC on streets than observed close to facades in our monitoring campaign, on average. It is of note that the instruments used for MM and our measurements have different cut-off ranges (>7 nm for CPC instrument used on-road in the CAV and 10-300 nm in facade-level measurements using the DM); thus, the absolute values might not be directly comparable, which is a limitation.

UFP measurements with DiSCminis

Several factors influenced the annual PNC means determined by our measurement campaign. Firstly, our method of temporal adjustment relies strongly on the annual mean measured at a reference site. To confirm whether our reference site measurements were representative of other locations, we found that daily variation reflected that at five municipal monitoring stations throughout the city. Moreover, we assessed the repeatability of DM instruments and found acceptable agreement between instruments when co-located for up to two weeks. Moreover, we have previously shown that the DM instruments can capture high on-road PNC levels in a personal monitoring study with bicycling participants (34). However, continuous monitoring at a reference site for one year with DMs proved challenging. Several instrument malfunctions led to missing data, such as due to pump malfunctioning or errors in the output files. Moreover, meteorological conditions, such as high temperatures during summer, as well

as humidity and precipitation, led to malfunctioning of the instrument or to unreliable values that were removed during data cleaning. Regular calibrations and a thorough data cleaning procedure were applied in order to ensure reliable data. Nonetheless, a large number of missing data could have affected the annual mean at the reference site, and subsequently annual means at monitoring sites. When considering the ‘raw’ monitored concentrations in each campaign separately, we saw better, but still low correlations of either value with CAV, potentially indicating issues related to temporal adjustment. We expect PNC at residential sites throughout the city to be temporally correlated with PNC at the reference site, with differences only in the absolute numbers. This was true for most sites, but some sites were weakly correlated with the reference site at hourly averages. This could be due to local sources of PNC or due to meteorological conditions, especially wind direction. In addition, we would expect the ratio of residential site PNC to reference site PNC to be similar in both campaigns, which was not the case for about half of the sites. This could have been improved by additional measurement campaigns, ideally four sampling periods per year and site, in order to capture each season. In terms of the practical sampling conditions, we used weather-proof plastic boxes, which were attached to windowsills, placed on balconies or in house entrances. This could possibly have influenced measured data, in the sense that less variation in PNC could be picked up by the instrument when placed close to a wall and with the inlet immediately close to a plastic box. In addition, instruments were placed facing the street wherever possible, with the exception of four sites, where they were placed in backyards/gardens. Even though those four sites were low-traffic sites, measured concentrations may not reflect those facing the street.

Generally, the calibration of instruments measuring PNC is characterized by a substantial uncertainty, which varies between 30% for lower concentrations (less than 1,000 pt/cm³) to 10% in a typical urban background (about 10,000 pt/cm³), based on standardized methodology (11). DM accuracy for measuring PNC is specified by the manufacturer with $\pm 30\%$, which has been confirmed in studies comparing DM to regulatory-grade SMPS or CPC instruments (35,36).

Measurement campaign UFP levels

The temporally adjusted annual means, based on the current measurement campaign of two measurements at 27 residential sites, were lower than those observed in other studies. One study, similar to ours, has estimated annual PNC based on 24-hour-measurements in three

seasons at residential sites in Switzerland and the Netherlands (37). They found considerably higher mean PNC ($\sim 12,000$ pt/cm³) at residential sites in both areas combined, than we found in our campaign (5,201 pt/cm³). Another study, where six-week-measurements were done at residential sites in two study areas in metropolitan Boston (MA, USA), found a mean PNC of 11,000 pt/cm³ (38). Similarly high levels were also seen in a Dutch study, where PNC was measured on sidewalks close to residential sites, and temporally adjusted, with a mean of $\sim 12,600$ pt/cm³ (29,32). The low concentrations observed in the present study are in line with the generally low levels of air pollution in Copenhagen as seen in routine monitoring (39). Worth mentioning here are Copenhagen's strategies for active mobility, with about half of Copenhagen's residents commuting to work or school by bicycle (40).

While other monitoring studies of PNC observed highest levels during winter (28,38,41), PNC was highest in spring, i.e. March-May, in the current study. This pattern has previously been observed in Copenhagen and could be explained by the increased photochemical activity during these months, initiating particle formation in the atmosphere (23).

Overestimation of UFP models

There could be several reasons for the overestimation of PNC by the CAV-model at our residential monitoring sites. Most importantly, Google Street View cars measured air pollution on-road, which could be up to a hundred meters away from residential sites, where we measured PNC at facades, balconies or in house entrances. UFP are characterized by their sharp decline with increasing distance to their sources (10,11), so levels are expected to be lower at residences than on roads. Similar to our results, a recent study found that PNC from the CAV-MM was about twice as high as 2019 annual mean PNC from three fixed-site regulatory monitoring stations in Copenhagen, even after applying corrections to their levels based on the different locations (on-road vs roadside) and timing (week-day/day-time vs annual mean) (26). Moreover, PNC predictions for residences have been found to be higher when a model was based on mobile monitoring compared to short-term stationary monitoring (30 minutes) in the Netherlands, both done by the same electric car and instruments. Here, stationary monitoring was done on sidewalks, closer to facades, while mobile monitoring was done on-road, by which predicted PNC was about 1.4 times higher for 12,682 residential addresses (29). Furthermore, we have used the same DM instruments as in the present study for personal exposure monitoring while bicycling a fixed 8.5 km route through Copenhagen in September and

October 2020, finding mean PNC of around 18,000 pt/cm³ directly next to streets with traffic, both during and outside rush-hours (34). In another personal monitoring study, using the DMs, during COVID-19 closures and re-openings from late-March to mid-July 2020, levels were found to be similar during bicycling but lower during walking, particularly in residential areas (42).

Another possible explanation for the discrepancy between monitored and modelled PNC is that concentrations have been decreasing continuously in Copenhagen since becoming included in routine measurements by the Danish National Air Quality Monitoring Programme at two monitoring stations in central Copenhagen in 2002. Annual concentrations were lower in 2021 than in 2019 (39), which could partly explain the absolute difference between Google Street View measurements in October 2018-March 2020 and our measurements from May 2021-May 2022. Another contributing factor are the different size ranges captured by DM (10-300 nm) and CPC (>7 nm) used in Google Street View measurements. According to best practice recommendations by the World Health Organization, especially the lower detection limit for particle size is critical in PNC measurements and should ideally be ≤ 10 nm (43). In terms of the upper limit of particle diameter, an open limit is recommended, because this is less critical since particle numbers are low for particle sizes well above 0.1 micrometer (11). With 7 nm, the CPC's lower detection limit is lower than the DM's with 10 nm. However, only a small fraction of measured particles is found in this size range, which is why this difference should not result in substantial differences in PNC.

Correlation between residential measurements and model predictions

Even with the expected differences in absolute levels between street- and facade-level, as well as decreasing levels of PNC in Copenhagen over the past years, we do not expect the spatial variation of PNC in Copenhagen to have changed to a degree that could explain the inexistent correlation between residential measurements and CAV. In Kerckhoff et al.'s study in the Netherlands, correlation between models based on mobile and short-term monitoring away from roads was high (0.89), even though absolute levels at residential sites were overestimated by mobile monitoring (29). However, in the present monitoring campaign, we did not see high correlation between monitored and modelled PNC based on mobile monitoring, which is unexpected and not in line with previous studies, especially in the Netherlands. There could be several explanations for this. Most importantly, we observed a small range of annual mean

PNC at residential sites in our measurement campaigns (3,735-6,588 pt/cm³), most likely related to a relatively low number of sites close to major roads. However, UFP concentrations and their range are generally low in Copenhagen, such as observed in the annual means at five municipality monitoring stations (range: 5,590-7,600 pt/cm³) and at street-level and background stations as part of the Danish Air Quality Monitoring Programme (23,39). Another factor are the previously described limitations in measurements, and estimation of annual means at sites. Thus, if we believe our monitored PNC to be inaccurate, we must conclude that spatial contrasts from CAV could not be validated by our monitoring campaign. If we believe the CAV-model to be inaccurate, this could reflect the challenges in modelling spatial variation of UFP based on mobile monitoring. In fact, the LUR-model for the CAV-model was able to explain 46% of variation in the monitored on-road UFP by the Google Street View car, which reflects the challenges in UFP modelling. Notably, the CAV-model predictions for nitrogen dioxide (NO₂) and black carbon (BC), which were not measured in the present study, have, in another study, been shown to be moderately correlated with existing European-wide LUR-model predictions for residential exposures. Correlation between both models' predictions of NO₂ and BC at 76,752 residences in Copenhagen were 0.55 and 0.38, respectively (44).

Few studies have attempted at validating PNC models by external measurements. Another model based on mobile measurements with Google Street View cars in the Netherlands in 2016-2017 has been validated by longer-term (24 h) measurements at 42 sites in three seasons each, and found to agree with an R² of 0.6 (25). In another study, a LUR-model for PNC was externally validated by 24-hour measurements at around 80 residential facades in Switzerland and the Netherlands, using DMs and temporal adjustment based on a reference site similar to the present study (19). They found moderate agreement between modelled and measured PNC (R²: 0.50-0.53), which is much higher than what was observed in our study. Others have compared central-site measurements (two years) to six-week-measurements at residential sites, as well as 42-day mobile measurements on a 40 km route, using CPCs (38). Like our study, they found highest levels by on-road monitoring. Additionally, they found the correlation between locations to be most affected by hour of the day, with better agreement at night and outside traffic rush-hours, and by wind direction. Sampling at irregular times of the day across different streets by the Google Street View cars might have introduced more noise to the observed data (as the response variable has been means of means in the LUR); thus, fixed terms of the LUR-model may not be well-suited to explain the noisy variations in the observed data, as R² reported to be 46%. Traffic patterns are most likely not distributed uniformly within the

study area, with some locations more affected by rush hours, and corresponding increases in UFP, than others.

Strengths and limitations

Strengths of our study include a thorough monitoring campaign of PNC at 37 residential sites with quality-controlled data throughout Copenhagen, including adjustment for seasonal and day-to-day variations based on a reference site. However, the study has several limitations. Firstly, during our monitoring campaign we experienced challenges in monitoring with DMs. While they are attractive for mobile UFP measurements due to their portability, simple operation, and lower cost than comparable instruments, they are very sensitive to temperature and humidity, and need frequent calibrations. Instrument malfunctions led to a relatively low number of monitoring sites and to missing data at the reference site. Thus, the number of observed locations might have been too small. We could not follow the manufacturer's recommendations of a lower temperature limit for DM measurements at 10°C, with temperatures being below this during most of our second campaign. While this did not lead to apparent instrument malfunctions, such as pump failures during high temperatures in summer, we are not able to explain whether this has influenced our measured data. Moreover, while the accuracy and precision evaluations showed mostly acceptable results based on the available data, except for questionable agreement with SMPS in one co-location and disagreement in absolute levels between two DMs in another (possible due to instrument drift), we could not compare all instruments due to instrument malfunctions. However, malfunctioning instruments were always returned to the manufacturer for servicing, and unreliable data was not included in our final data. Next, for comparison to model predictions by the CAV-model, there were limitations in comparability, such as from differences in location (on-road vs residences), timing (2018-2020 vs 2021-2022), measurement methods (mobile monitoring vs fixed sites), instruments, or approach in averaging values (no adjustment vs temporally adjusted annual means). Nonetheless, we do not expect any of these factors to result in systematic disagreement between the modelled and measured concentrations, as seen in our study.

5. Conclusions

In summary, we found that overall, residential facade-level measurements were not correlated with CAV-model predictions of UFP at 27 sites in Copenhagen. These results need to be interpreted with caution due to the presence of several methodological limitations in measured data. Very low number of traffic sites among 37 residential locations in part explains the lack of correlation, as CAV-model is based on traffic-related UFPs Google Air View measurements and would not be predict well sites where UFPs come from various sources. We conclude that the findings presented here, do not support the use of CAV for residential exposure assessment in health studies of UFP at this time. Further understanding of CAV is needed, such as by additional external model validation at more sites with a larger range of exposure levels, with standardized instruments and monitoring methods.

Acknowledgements

This work was supported by Health Effects Institute (HEI) (#4982-RFA19-2/21-5) and Novo Nordisk Foundation Challenge Programme (NNF17OC0027812). Research described in this article was conducted under contract to the HEI, an organization jointly funded by the United States Environmental Protection Agency (EPA) (Assistance Award CR 83998101) and certain motor vehicle and engine manufacturers. The contents of this article do not necessarily reflect the views of HEI, or its sponsors, nor do they necessarily reflect the views and policies of the EPA or motor vehicle and engine manufacturers.

References

1. Murray CJL, Aravkin AY, Zheng P, Abbafati C, Abbas KM, Abbasi-Kangevari M, et al. Global burden of 87 risk factors in 204 countries and territories, 1990–2019: a systematic analysis for the Global Burden of Disease Study 2019. *The Lancet*. 2020 Oct 17;396(10258):1223–49.
2. Ellermann T, Nygaard J, Nøjgaard JK, Nordstrøm C, Brandt J, Christensen J, et al. The Danish Air Quality Monitoring Programme. Annual Summary for 2018. Copenhagen: Aarhus University, DCE – Danish Centre for Environment and Energy; 2020.
3. Health Effects Institute. State of Global Air 2020. Special Report. Boston, MA: Health Effects Institute; 2020.
4. European Environment Agency. Air quality in Europe - 2020 report — European Environment Agency [Internet]. Luxembourg: Publications Office of the European Union; 2020 [cited 2021 Jun 8]. Report No.: 9/2020. Available from: <https://www.eea.europa.eu/publications/air-quality-in-europe-2020-report>
5. Schraufnagel DE. The health effects of ultrafine particles. *Exp Mol Med*. 2020 Mar;52(3):311–7.
6. Ohlwein S, Kappeler R, Kutlar Joss M, Künzli N, Hoffmann B. Health effects of ultrafine particles: a systematic literature review update of epidemiological evidence. *Int J Public Health*. 2019 May;64(4):547–59.
7. Kwon HS, Ryu MH, Carlsten C. Ultrafine particles: unique physicochemical properties relevant to health and disease. *Exp Mol Med*. 2020 Mar 17;52(3):318–28.
8. Moreno-Ríos AL, Tejada-Benítez LP, Bustillo-Lecompte CF. Sources, characteristics, toxicity, and control of ultrafine particles: An overview. *Geosci Front*. 2021 Jan 20;101147.
9. Hofman J, Staelens J, Cordell R, Stroobants C, Zikova N, Hama SML, et al. Ultrafine particles in four European urban environments: Results from a new continuous long-term monitoring network. *Atmos Environ*. 2016 Jul 1;136:68–81.
10. de Nazelle A, Bode O, Orjuela JP. Comparison of air pollution exposures in active vs. passive travel modes in European cities: A quantitative review. *Environ Int*. 2017 Feb;99:151–60.
11. Morawska L, Wierzbicka A, Buonanno G, Cyrus J, Schnelle-Kreis J, Kowalski M, et al. Ambient ultrafine particles: evidence for policy makers. A report prepared by the ‘Thinking outside the box’ team [Internet]. 2019 [cited 2020 Jul 12]. Available from: [https://efca.net/files/WHITE%20PAPER-UFP%20evidence%20for%20policy%20makers%20\(25%20OCT\).pdf](https://efca.net/files/WHITE%20PAPER-UFP%20evidence%20for%20policy%20makers%20(25%20OCT).pdf)
12. Abernethy RC, Allen RW, McKendry IG, Brauer M. A Land Use Regression Model for Ultrafine Particles in Vancouver, Canada. *Environ Sci Technol*. 2013 May 21;47(10):5217–25.
13. Eeftens M, Meier R, Schindler C, Aguilera I, Phuleria H, Ineichen A, et al. Development of land use regression models for nitrogen dioxide, ultrafine particles, lung deposited surface area, and four other markers of particulate matter pollution in the Swiss SAPALDIA regions. *Environ Health*. 2016 Apr 18;15:53.
14. Hankey S, Marshall JD. Land Use Regression Models of On-Road Particulate Air Pollution (Particle Number, Black Carbon, PM_{2.5}, Particle Size) Using Mobile Monitoring. *Environ Sci Technol*. 2015 Aug 4;49(15):9194–202.

15. Hoek G, Beelen R, Kos G, Dijkema M, Zee SC van der, Fischer PH, et al. Land Use Regression Model for Ultrafine Particles in Amsterdam. *Environ Sci Technol*. 2011 Jan 15;45(2):622–8.
16. Jones RR, Hoek G, Fisher JA, Hasheminassab S, Wang D, Ward MH, et al. Land use regression models for ultrafine particles, fine particles, and black carbon in Southern California. *Sci Total Environ*. 2020 Jan 10;699:134234.
17. Sabaliauskas K, Jeong CH, Yao X, Reali C, Sun T, Evans GJ. Development of a land-use regression model for ultrafine particles in Toronto, Canada. *Atmos Environ*. 2015 Jun;110:84–92.
18. Saraswat A, Apte JS, Kandlikar M, Brauer M, Henderson SB, Marshall JD. Spatiotemporal Land Use Regression Models of Fine, Ultrafine, and Black Carbon Particulate Matter in New Delhi, India. *Environ Sci Technol*. 2013 Nov 19;47(22):12903–11.
19. van Nunen E, Vermeulen R, Tsai MY, Probst-Hensch N, Ineichen A, Davey M, et al. Land Use Regression Models for Ultrafine Particles in Six European Areas. *Environ Sci Technol*. 2017 Mar 21;51(6):3336–45.
20. Wolf K, Cyrus J, Hrciníková T, Gu J, Kusch T, Hampel R, et al. Land use regression modeling of ultrafine particles, ozone, nitrogen oxides and markers of particulate matter pollution in Augsburg, Germany. *Sci Total Environ*. 2017 Feb 1;579:1531–40.
21. Ryan PH, LeMasters GK. A Review of Land-use Regression Models for Characterizing Intraurban Air Pollution Exposure. *Inhal Toxicol*. 2007;19(Suppl 1):127–33.
22. Kerckhoffs J, Khan J, Hoek G, Yuan Z, Hertel O, Ketznel M, et al. Hyperlocal variation of nitrogen dioxide, black carbon, and ultrafine particles measured with Google Street View cars in Amsterdam and Copenhagen. *Environ Int*. 2022 Dec 1;170:107575.
23. Ellermann T, Massling A, Bossi R, Nordstrøm C. The Particle Project 2021 [Internet]. Aarhus University, DCE – Danish Centre for Environment and Energy; 2022 [cited 2023 Jan 19] p. 38. (Scientific Report from DCE – Danish Centre for Environment and Energy No. 500). Available from: <https://dce2.au.dk/pub/SR500.pdf>
24. Jensen SS, Ketznel M, Khan J, Valencia VH, Brandt J, Christensen JH, et al. Luften på din vej 2.0. Nationalt Center for Miljø og Energi; 2021 p. 62. (Videnskabelig rapport fra DCE). Report No.: 445.
25. Kerckhoffs J, Hoek G, Gehring U, Vermeulen R. Modelling nationwide spatial variation of ultrafine particles based on mobile monitoring. *Environ Int*. 2021 Sep 1;154:106569.
26. Ellermann T, Khan J, Ketznel M, Jensen SS, Hertel O. Air View Data on the spatial distribution of air pollution in Copenhagen [Internet]. 2021 p. 27. Report No.: Scientific note no. 2021, 40. Available from: https://dce.au.dk/fileadmin/dce.au.dk/Udgivelser/Notater_2021/N2021_40.pdf
27. Kerckhoffs J, Khan J, Hoek G, Yuan Z, Ellermann T, Hertel O, et al. Mixed-Effects Modeling Framework for Amsterdam and Copenhagen for Outdoor NO₂ Concentrations Using Measurements Sampled with Google Street View Cars. *Environ Sci Technol*. 2022 Jun 7;56(11):7174–84.
28. Eeftens M, Phuleria HC, Meier R, Aguilera I, Corradi E, Davey M, et al. Spatial and temporal variability of ultrafine particles, NO₂, PM_{2.5}, PM_{2.5} absorbance, PM₁₀ and PM_{coarse} in Swiss study areas. *Atmos Environ*. 2015 Jun 1;111:60–70.

29. Kerckhoffs J, Hoek G, Messier KP, Brunekreef B, Meliefste K, Klompmaker JO, et al. Comparison of Ultrafine Particle and Black Carbon Concentration Predictions from a Mobile and Short-Term Stationary Land-Use Regression Model. *Environ Sci Technol*. 2016 Dec 6;50(23):12894–902.
30. Statens Serum Institut. Tidslinje for covid-19 [Internet]. 2022 [cited 2023 Feb 22]. Available from: <https://www.ssi.dk/-/media/arkiv/subsites/covid19/presse/tidslinje-over-covid-19/covid-19-tidslinje-lang-for-2020-2022-version-2---december-2022.pdf>
31. Eeftens M, Tsai MY, Ampe C, Anwander B, Beelen R, Bellander T, et al. Spatial variation of PM_{2.5}, PM₁₀, PM_{2.5} absorbance and PM_{coarse} concentrations between and within 20 European study areas and the relationship with NO₂ – Results of the ESCAPE project. *Atmos Environ*. 2012 Dec 1;62:303–17.
32. Klompmaker JO, Montagne DR, Meliefste K, Hoek G, Brunekreef B. Spatial variation of ultrafine particles and black carbon in two cities: Results from a short-term measurement campaign. *Sci Total Environ*. 2015 Mar 1;508:266–75.
33. Sibson R. A brief description of natural neighbor interpolation. In: Barnett, V (Ed), *Interpreting Multivariate Data* [Internet]. New York, NY: John Wiley & Sons, Inc.; 1981 [cited 2023 Jan 24]. p. 21–36. Available from: <https://www.semanticscholar.org/paper/A-brief-description-of-natural-neighbor-Sibson/1ca6926bf459db0a4d89a8c88b9fd64c32760bc2>
34. Bergmann ML, Andersen ZJ, Amini H, Khan J, Lim YH, Loft S, et al. Ultrafine particle exposure for bicycle commutes in rush and non-rush hour traffic: A repeated measures study in Copenhagen, Denmark. *Environ Pollut*. 2022 Feb 1;294:118631.
35. Kaminski H, Kuhlbusch TAJ, Rath S, Götz U, Sprenger M, Wels D, et al. Comparability of mobility particle sizers and diffusion chargers. *J Aerosol Sci*. 2013 Mar 1;57:156–78.
36. Mills JB, Park JH, Peters TM. Comparison of the DiSCmini aerosol monitor to a handheld condensation particle counter and a scanning mobility particle sizer for submicrometer sodium chloride and metal aerosols. *J Occup Environ Hyg*. 2013;10(5):250–8.
37. van Nunen E, Vermeulen R, Tsai MY, Probst-Hensch N, Ineichen A, Imboden M, et al. Associations between modeled residential outdoor and measured personal exposure to ultrafine particles in four European study areas. *Atmos Environ*. 2020 Apr 1;226:117353.
38. Simon MC, Hudda N, Naumova EN, Levy JI, Brugge D, Durant JL. Comparisons of Traffic-Related Ultrafine Particle Number Concentrations Measured in Two Urban Areas by Central, Residential, and Mobile Monitoring. *Atmospheric Environ Oxf Engl* 1994. 2017 Nov;169:113–27.
39. Ellermann T, Nordstrøm C, Massling A, Sørensen MB. Status for måling af luftkvalitet i 2021 [Internet]. Aarhus Universitet, DCE - Nationalt Center for Miljø og Energi; 2022 [cited 2022 Jul 29] p. 25. (Teknisk rapport fra DCE – Nationalt Center for Miljø og Energi). Report No.: Teknisk rapport nr. 245. Available from: <https://dce2.au.dk/pub/TR245.pdf>
40. City of Copenhagen, Technical and Environmental Administration, (TMF), Mobility. The Bicycle Account 2018. Copenhagen City of Cyclists [Internet]. 2019 [cited 2021 May 31]. Available from: https://kk.sites.itera.dk/apps/kk_pub2/index.asp?mode=detalje&id=1962
41. Ragettli MS, Ducret-Stich RE, Foraster M, Morelli X, Aguilera I, Basagaña X, et al. Spatio-temporal variation of urban ultrafine particle number concentrations. *Atmos Environ*. 2014 Oct 1;96:275–83.

42. Bergmann ML, Andersen ZJ, Amini H, Ellermann T, Hertel O, Lim YH, et al. Exposure to ultrafine particles while walking or bicycling during COVID-19 closures: A repeated measures study in Copenhagen, Denmark. *Sci Total Environ.* 2021 Oct 15;791:148301.
43. World Health Organization. WHO global air quality guidelines: particulate matter (PM_{2.5} and PM₁₀), ozone, nitrogen dioxide, sulfur dioxide and carbon monoxide [Internet]. World Health Organization; 2021 [cited 2021 Dec 10]. xxi, 273 p. Available from: <https://apps.who.int/iris/handle/10665/345329>
44. Tayebi S, Kerckhoffs J, Khan J, de Hoogh K, Chen J, Shahri SMT, et al. Comparing Street- and Residential-level Nitrogen Dioxide and Black Carbon Concentrations Estimated Using Google Street View-based and Conventional European-wide LUR Models in Copenhagen, Denmark. 2023;